Boosted Thermoelectric Properties of Low-density Polymer Bulk Prepared by Spark Plasma Sintering

Zhen-Hua Ge, Yi Chang, Fu Li [a, *], Jingting Lou, Ping Fan

1. Experimental Section

The following process was adopted for the fabrication of polymer/inorganic composite bulk. Poly(3,4-ethylenedioxythiophene)-poly(styrenesulfonate) (PEDOT:PSS, 3-4% in water) we used in this work was purchased from ALORICH without any further processing. The synthesis process is shown in Fig. 1(a), the 33.33 wt% ratio of inorganic powders (Bi_2S_3 nanotubes[28], Cu_2SnSe_3 nanoparticles[29], and $Bi_{0.5}Sb_{1.5}Te_3$ powders with dimensions under 400 meshes were obtained by ground the alloy ingot) were mixed with PEDOT:PSS by ultrasonic for 6 h. The mixed solution was then put on the Al plates for drying at 40 °C for 12h in oven. The PEDOT:PSS/inorganic powders pieces were obtained and then grounded in the liquid nitrogen to fine composite powders. The PEDOT:PSS/inorganic powders fine powder was dried again in vacuum oven at room temperature for 12 h. The PEDOT:PSS/inorganic powders fine powder was then densified by employing spark plasma sintering (SPS) using custom-designed 10 mm diameter graphite die resulted in a pellet. The optimized SPS parameters used were 50MPa, a 50°C/min ramp rate and a holding time of 5 min at 100 ℃ under vacuum (<4 MPa).

The as-synthesized PEDOT:PSS/inorganic powders bulk, as shown in Figure 1(b), were characterized by X-ray diffraction (XRD) and scanning electron microscopy (SEM, JEOL JSM 6390 LV). Electrical conductivity and thermopower/Seebeck coefficient were measured on polished parallelepipeds approximately 2×2×8 mm in an ULVAC ZEM-3 electrical conductivity and Seebeck coefficient system. Samples were sandwiched between two Ni electrodes with two probe thermocouples providing forced contacts on one side. A resistive heater on the lower electrode provided nominal temperature differentials of 10, 20, and 30℃ to determine the Seebeck coefficient. The sample chamber was evacuated and back filled with approximately 0.1 atm He, and heated from room temperature to 75℃ using an IR furnace. Thermal diffusivity and specific heat of samples were measured on a Netzsch LFA 457. Coins measuring approximately 8 mm in diameter by 1 mm thickness were heated from room temperature to 950 K. Density was calculated from the sample dimensions and mass. Assuming the law of mixtures, specific heat of the samples was estimated using established literature values for corresponding ideal mixtures of PEDOT:PSS and inorganic powders. [1, 2] Total thermal conductivity was calculated using the equation $k = DC_p d$, where k is total thermal conductivity, D is measured thermal diffusivity, C_p is specific heat, and d is density. The Hall coefficients at room temperatures were measured using the Van der Pauw technique under a reversible magnetic field of 0.80 T (Lake Shore 8400 Series, Model 8404, USA). The TGA-DSC was analyzed using simultaneous thermal analyzer (STA 447, Netzsch, Germany) under Ar flow. The room temperature optical absorption spectrum was measured using sintered polymer bulk. The measurement was performed on UV-vis Spectrophotometer (Shimadzu,

2. DSC-TG

Figure S1 shows the DSC and TG curves for all polymer composites samples from 20 to 200 ^{o}C. As shown Figure S1(a), there is a bump around 80-90 ^{o}C in all curves, this temperature was considered to be the softening temperature, this is also the reason that the polymer powder could reform to polymer bulk under the sintering temperature 100 ^{o}C. The TG curves of all the samples kept flat and slightly decreased, showing no heavy weight loss. The DSC result was also shown in Figure 2 in the revised manuscript, the related discussion was added either.
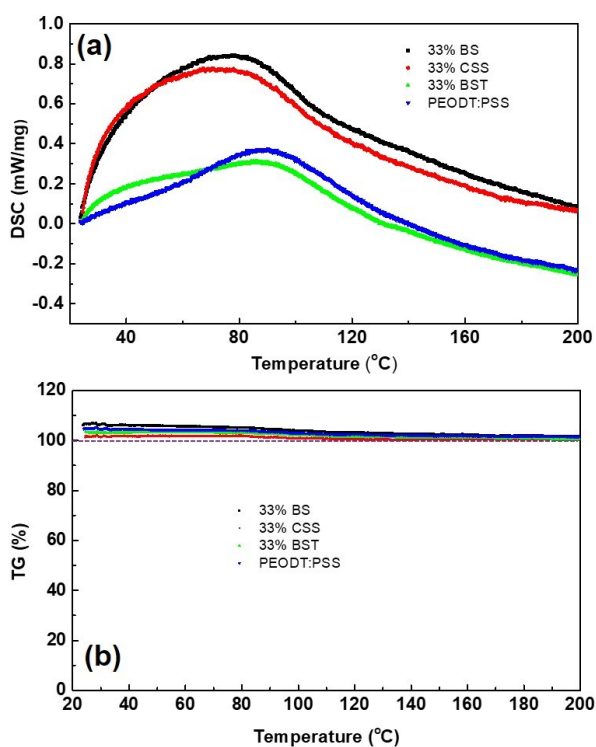

Figure S1 DSC and TG curves for all polymer composites samples from 20 to 200 ^{o}C.

3. EDS mapping

EDS mapping in SEM was performed for all the polymer composites samples. To make sure that the scanning surface is flat enough, the free surface was used instead of fracture surface. The results

were added in the ESI part as Figure S2, Figure S3 and Figure S4. As shown in Figures S2, S3, and S4,
same particles distributed on the surface, but lots of them embed in the PEDOT:PSS matrix. The
distribution of Cu_2SnSe_3 nanoparticles are the most homogeneous compared to that of the other two
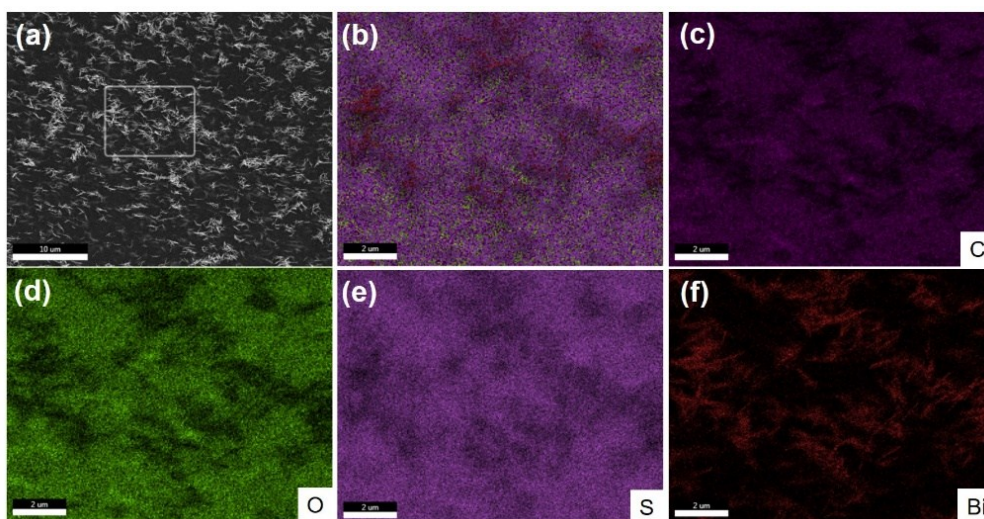samples.

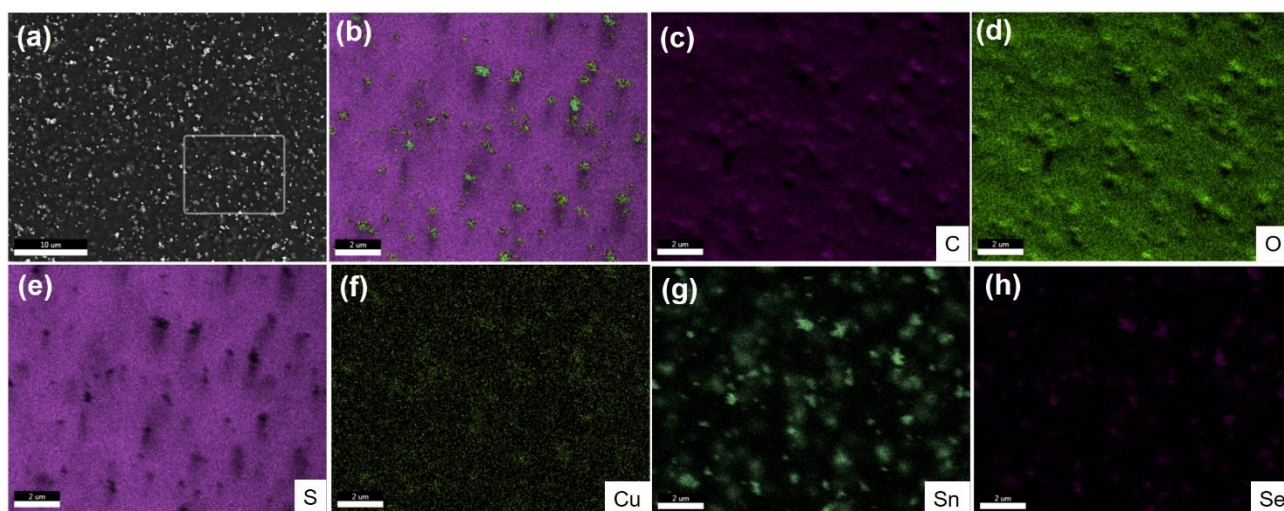Figure S2 EDS mapping of PEODT:PSS with 33 wt% Bi_2S_3 nanotubes

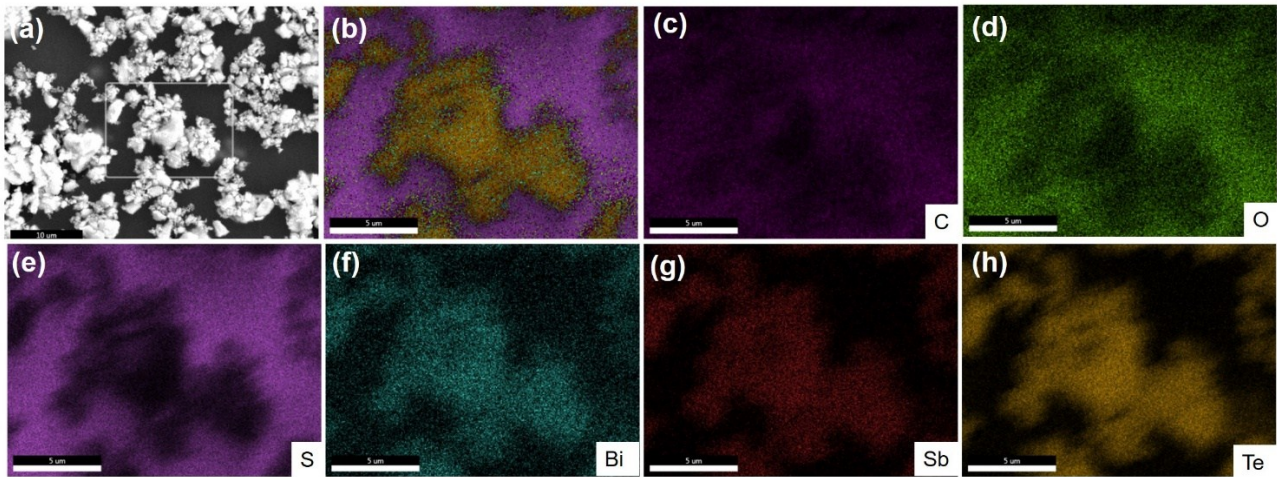Figure S3 EDS mapping of PEODT:PSS with 33 wt% Cu_2SnSe_3 nanoparticles

Figure S4 EDS mapping of PEODT:PSS with 33 wt% $Bi_{0.5}Sb_{1.5}Te_3$ powders.

4. UV-vis-near IR

Figure S5 show an obvious absorption edge around the wave length of 1650 nm, the simply estimated

band gap of polymer bulk is 0.75 eV by using Eg=1240/λ, where λ is wave length. The band gap of

0.75 eV is a little lower than the reported band gap of PEDOT:PSS films from 1.07 to 1.63 depending

on the different substrates. [6] The other two absorption peaks were also observed around 750 to

800 nm, which is according to the band gap of around 1.2 to 1.4[7, 8] for Bi_2S_3 and Cu_2SnSe_3. The

BiSbTe is a norrow band semiconductor with a band gap of below 0.3 [9], it is therefore no absorption

peak was detected in the wave length ranges from 190 to 1800 nm. And the FI spectrometer is not

available in our lab. We may report the FI reflectance spectrum for 33%BST sample in the future.
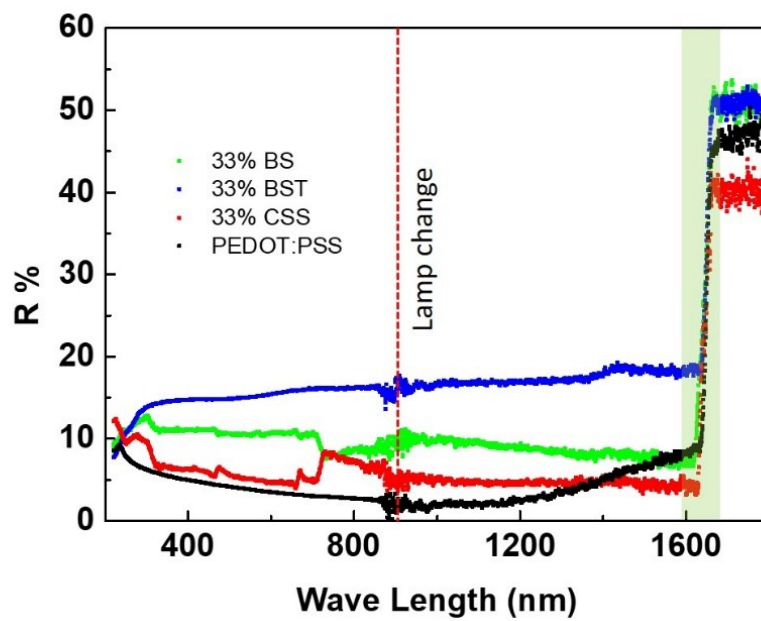
Figure S5 UV-vis-near IR reflectance spectrum for all the polymer composites bulk.

Table S1: Thermoelectric properties of selected organic semiconductor

Materials	Conductivity [S/m]	Seebeck [µV/K]	Power factor [W/m-K2]	Thermal cond [W/m-K]	ZT	Processing	Ref
Pristine PEDOT:PSS bulk	1474	20	6.8×10^{-7}	0.10	2×10^{-3}	Hot press, ZT was obtained at 348 K	This work
33 wt% BST with PEDOT:PSS	2070	28	1.4×10^{-6}	0.08	6×10^{-3}	Hot press ZT was obtained at 348 K	This work
33 wt% CSS with PEDOT:PSS	2762	57	1.1×10^{-5}	0.08	0.04	Hot press ZT was obtained at 348 K	This work
P(NDIOD-T2) with N-DMBI	4×10^{-3}	-770	2×10^{-7}	-	-	Doped in solution and spin cast	Schlitz et al. [5]
P(NDIOD-T2) with N-DPBI	8×10^{-3}	-850	6×10^{-7}	-	-	Doped in solution and spin cast	Schlitz et al. [5]
Polyaniline	6.3	-3	5.7×10^{-9}	-	-	Vapor doped with H_2SO_4	Yoon et al. [10]
Poly[Kx(Ni-ett)]	40	-122	6×10^{-5}	-	-	Solid-state processing	Sun et al. [11]
P3HT doped with PF_6	0.843	39	1.4×10^{-7}	-	-	Electrochemical doping of film drop cast from solution	Xuan et al. [12]
PEDOT:PSS film	72.6	895	4.72×10^{-3}	0.22	0.42	spin cast and dip in EG solution	Kim et al. [13]
P3HT/SW-CNT composites	10000	-29	9.5×10^{-4}	0.16	$>10^{-2}$	Cold press densification	Bounioux et al. [14]
PEDOT:PSS	800	15.5	1.9×10^{-7}	0.04~0.16	3×10^{-4}	Cold press densification	Jiang et al. [15]
PEDOT:PSS with DMSO	5500	13	9×10^{-7}	0.04~0.16	1.8×10^{-3}	Cold press densification	Jiang et al. [15]
PEDOT:PSS film	132	18.9	5×10^{-8}	0.22-0.30	6×10^{-5}	Drop cast	See et al. [16]
PEDOT:PSS/Te NWs	1930	163	7×10^{-5}	0.22-0.30	0.1	Drop cast	See et al. [16]
PEDOT:PSS/Bi2Te3	42100	18.6	9.9×10^{-6}	0.07	0.04	physical mixing method	Song et al. [17]
PEDOT:PSS/Bi2Te3	90000	25	4.7×10^{-5}	-	-	drop cast, Bi_2Te_3 was prepared by ball milling	Zhang et al. [18]

Notes and references

1 Z. H. Ge, B. P. Zhang, Z. X. Yu, B. B. Jiang, CrystEngComm, 2012, 14(6): 2283-2288.
2 Z. H. Ge, G. S. Nolas, Inorg. Chem., 2014, 53 (9), 4445-4449.
3 H. Park, S. H. Lee, F. S. Kim, H. H. Choi, I. W. Cheong, J. H. Kim, J. Mater. Chem. A2014, 2,6532.
4 Q. Jiang, H. Yan, J. Khaliq, H. Ning, S. Grasso, K. Simpson M. J. Reece, J. Mater. Chem. A2014, 2,5785.
5 R. A. Schlitz, F. G. Brunetti, A. M. Glaudell, P. L. Miller, M. A. Brady, C. J. Takacs, C. J. Hawker and M. L. Chabinycet, Adv. Mater., 2014, 26, 2825-2830.
6 L. Chen, X.J. Wang, A. Govindasamy, H. Tsuboi, M. Koyama, M. Kubo, A. Miyamoto, Extended Abstracts of the 2004 International Conference on Solid State Devices and Materials, Tokyo, 2004, pp. 170-171.
7 G. Konstantatos, L. Levina, J. Tang, E.H. Sargent, *Nano Lett.*, 2008, **8**, 4002-4006.
8 M. Ahmadi, S. S. Pramana, S. K. Batabyal, C. Boothroyd, S.G. Mhaisalkar, Y.M. Lam, *Inorg. Chem.*, 2013, **52**, 1722-1728.
9 B.Y. Yavorsky, N.F. Hinsche, I. Mertig, P. Zahn, *Phys. Rev. B.*, 2011, **84**, 165208
10
11 C. O. Yoon, M. Reghu, D. Moses D, A. J. Heeger, Y. Cao, T.-A. Chen, X. Wu and R. D. *Rieke, Synthetic Met.*, **1995**, 75, 229-239.
12 Y. M. Sun, P. Sheng, C. A. Di, F. Jiao, W. Xu, D. Qiu and D. B. Zhu, Adv. Mater., 2012, 24, 932-937.
13 Y. Xuan, X. Liu, S. Desbief, P. Leclère, M. Fahlman, R. Lazzaroni, M. Berggren, J. Cornil, D. Emin, and X. Crispin, Phys. Rev. B, 2010, 82, 115454.
14 G. H. Kim, L. Shao, K. Zhang and K. P. Pipe, Nat. Mater., 2013, 12, 719-723.
15 C. Bounioux, P. Díaz-Chao, M. Campoy-Quiles, M. S. Martín-González, A. R. Goñi, R. Yerushalmi-Rozen and C. Müller, Energy Environ. Sci., 2013, 6, 918-925.
16 F. X. Jiang, J. K. Xu, B. Y. Lu, Y. Xie, R. J. Huang and L. F. Li, Chin. Phys. Lett., 2008, 25, 2202.
17 K. C. See, J. P. Feser, C.E. Chen, A. Majumdar, J. J. Urban and R. A. Segalman, Nano Lett., 2010, 10, 4664-4667.
18 H. J. Song, C. C. Liu, H. F. Zhu, F. F. Kong, B. Y. Lu, J. K. Xu, J. M. Wang and F. Zhao, J. Electron. Mater. 2013, 46, 1268.
19 B. Zhang, J. Sun, H. E. Katz, F. Fang and R. L. Opila, ACS Appl. Mater. Inter., 2010, 2, 3170-3178.